A Density Functional Study of the Vibrations of Three Oligomers of Thiophene

Alessandra Degli Esposti

Istituto di Spettroscopia Molecolare - C. N. R., Via Gobetti, 101, 40129 Bologna, Italy

Francesco Zerbetto*

Dipartimento di Chimica "G. Ciamician", Università degli Studi di Bologna, Via F. Selmi 2, 40126 Bologna, Italy

Received: April 10, 1997; In Final Form: July 2, 1997[⊗]

The accuracy of two density functional derived models—BLYP/6-31G* and B3LYP/6-31G*—is tested to calculate the molecular response to slow neutrons and infrared photons in a series of oligomers of thiophene. In the first type of experiment, the response is a function of the vibrational frequencies and the shapes of the normal modes; in the second, knowledge of the dipole moment surface is also necessary. The combination of the two simulations allows one to conclude that both models give fairly accurate vibrational frequencies and normal modes but may overestimate the infrared response in large systems. For this spectroscopy, BLYP/6-31G* and B3LYP/6-31G* find all the modes present in the experiment to be active. A few modes with modest activity are also calculated to appear strongly in the spectrum. Scaling of the force fields shows the complementary roles of the two methods. BLYP/6-31G* is very accurate—scaling factor of 1.00—in the calculation of the $C_\alpha-C_\beta$, $C_\alpha-C_\alpha$, and HCC force constants, and B3LYP/6-31G* does not require scaling of CS, SCC, CCC, and CSC force constants. On the basis of the combined use of the two models, a simple procedure is proposed that should give good agreement with experimental results of conjugated systems.

1. Introduction

The link between molecular structure and properties is most apparent in quantum chemical calculations where any property cannot be calculated without knowledge of the geometrical information of the molecule. The progress of various computational techniques has made possible the reasonably accurate calculation of bond lengths and bond angles for well more than a decade. Somewhat slower has been the progress on other observables. The advent in chemistry of methodologies based on density functional theory,[1] and their upgrade through gradient corrections, has recently allowed the accurate nearly-routine calculation of several physical quantities. One of the most impressive achievements of recent years concerns the vibrational frequencies for which a statistical analysis of differences between experiment and theory has reported a deviation of the order of 1%.[2] Concerning the response of a molecule to an external stimulus, the simulation of its energy dependence—that is, the determination of energy levels—may fall short of the full target if not accompanied by a calculation of its intensities/cross sections. The spectroscopic interest in the theoretical estimate of the intensities is particularly evident for large molecules where more than one vibrational frequency can exist in a small energy range: without the knowledge of the intensities, misassignments can easily occur. A more practical reason to pursue the evaluation of the intensity distribution of the molecular response to an external stimulus lies in the use of spectral signatures to check the purity—or the modifications of a material—when it is used for the fabrication of precompetitive devices.[3] In this work, we try to assess the performance of two widely used models for the calculation, in a class of molecules, of the response to two different external stimuli, namely infrared radiation and slow neutrons. The two techniques are complementary, both because of the existence of selection rules in infrared and the lack of them in neutron scattering and because of the different quantities that enter the definition of the response. The molecules selected by us are α-2T, α-4T, and α-6T, three oligomers of thiophene whose technological interest has been increased by the recently documented silicon-like performance in thin-film transistors of α-6T.[4] For these systems, we recently reported[5] that the infrared, Raman, and inelastic neutron scattering (INS) spectra can be simulated with very good accuracy if the *ab initio* force field, calculated by the Hartree−Fock procedure in conjunction with the 3-21G* basis set (or 6-31G* for the two smaller isomers), is scaled by a small set of parameters common to the three molecules. The simulation depends critically on the correlation between experimental and calculated frequencies. For stretching vibrations, the difference between the two can exceed 200 cm^{-1}. These differences are hardly systematic and, depending on the number of vibrations, inversions in the assignments can occur. The availability of more accurate methods lowers the degree of uncertainty in the empirical process of frequency assignment.

The models we intend to test are the density functional with gradient corrections known as BLYP[6] and the hybrid Hartree−Fock density functional procedure known as B3LYP.[7] The test is carried out in steps: first we perform the simulation of the infrared and inelastic neutron scattering spectra. Attention is paid both to frequencies and intensities. Then we verify the validity of the vibrational assignment of our previous work. Finally, we scale the vibrational force fields to improve the agreement between experiment and theory. This allows us to emphasize intrinsic weaknesses and strong points of the two models.

2. Computational Background

A. *Ab Initio* Calculations. All the geometry optimizations and the subsequent force field calculations were performed with the Gaussian 94 suite of programs.[8] This release of the program overcomes the convergence problems that we encountered with

[⊗] Abstract published in *Advance ACS Abstracts,* August 15, 1997.

S1089-5639(97)01233-4 CCC: $14.00

TABLE 1: Optimized Structural Parameters of α-2T, α-4T, and α-6T. Labels I, II, and III Refer to BLYP/6-31G*, B3LYP/6-31G*, and HF/6-31G* Levels

	α-2T(I)	α-2T(II)	α-2T(III)	α-4T(I)	α-4T(II)	α-4T(III)	α-6T(I)	α-6T(II)	α-6T(III)	α-6T(expt)
$C_1C_{1'}$	1.4535	1.4512	1.4648	1.4432	1.4434	1.4617	1.4411	1.4415	1.4615	1.445(9)
C_3C_8				1.4476	1.4469	1.4632	1.4418	1.4422	1.4616	1.45(1)−1.46(1)
$C_{11}C_{15}$							1.4473	1.4470	1.4632	1.45(1)
C_1S_2	1.7798	1.7564	1.7391	1.7817	1.7578	1.7390	1.7824	1.7585	1.7390	1.730(7)−1.731(7)
S_2C_3	1.7535	1.7354	1.7250	1.7802	1.7568	1.7388	1.7819	1.7581	1.7389	1.733(8)−1.739(8)
$C_{11}S_{12}$				1.7534	1.7354	1.7249	1.7802	1.7565	1.7387	1.729(7)−1.733(7)
C_8S_{12}				1.7819	1.7576	1.7393	1.7821	1.7579	1.7389	1.733(7)−1.742(8)
$C_{15}S_{16}$							1.7820	1.7575	1.7392	1.719(8)−1.726(8)
$C_{17}S_{16}$							1.7531	1.7353	1.7248	1.704(9)−1.711(9)
C_1C_5	1.3911	1.3778	1.3515	1.3956	1.3807	1.3516	1.3972	1.3818	1.3518	1.37(1)−1.38(1)
C_3C_4	1.3791	1.3675	1.3444	1.3945	1.3797	1.3513	1.3971	1.3816	1.3518	1.36(1)
C_8C_9				1.3936	1.3794	1.3520	1.3963	1.3812	1.3517	1.36(1)
$C_{10}C_{11}$				1.3796	1.3678	1.3445	1.3949	1.3800	1.3513	1.38(1)
$C_{15}C_{19}$							1.3937	1.3795	1.3520	1.38(1)−1.40(1)
$C_{17}C_{18}$							1.3797	1.3679	1.3445	1.31(1)−1.32(1)
C_4C_5	1.4303	1.4243	1.4336	1.4189	1.4156	1.4294	1.4167	1.4138	1.4289	1.40(1)−1.41(1)
C_9C_{10}				1.4287	1.4233	1.4332	1.4183	1.4152	1.4293	1.40(1)
$C_{18}C_{19}$							1.4285	1.4232	1.4332	1.41(1)−1.42(1)
C_5H_6	1.0921	1.0849	1.0736	1.0920	1.0849	1.0735	1.0920	1.0849	1.0735	
C_4H_7	1.0919	1.0846	1.0734	1.0921	1.0849	1.0735	1.0920	1.0848	1.0735	
C_9H_{13}				1.0920	1.0849	1.0736	1.0920	1.0849	1.0736	
$C_{10}H_{14}$				1.0918		1.0733	1.0920	1.0845	1.0735	
$C_{19}H_{20}$							1.0920	1.0849	1.0736	
$C_{18}H_{21}$							1.0918	1.0845	1.0733	
C_xH_y[b]	1.0886	1.0816	1.0710	1.0885	1.0816	1.0709	1.0885	1.0816	1.0709	
$C_5C_1C_{1'}$	129.54	129.12	128.29	129.53	129.17	128.41	129.49	129.15	128.40	128.7(7)−128.7(6)
$S_2C_1C_{1'}$	120.65	120.76	120.95	120.70	120.76	120.87	120.73	120.80	120.86	120.9(5)
$S_2C_3C_4$	111.58	111.60	111.84	109.83	110.13	110.74	109.80	110.07	110.73	110.5(6)−111.3(6)
$C_1S_2C_3$	91.65	91.80	91.58	92.01	92.13	91.88	91.97	92.12	91.87	91.9(4)−91.8(4)
$C_3C_4C_5$	113.09	112.89	112.63	114.22	113.84	113.32	114.23	113.87	113.32	113.4(7)−113.8(7)
$S_2C_3C_8$				120.64	120.68	120.84	120.70	120.78	120.85	119.6(6)−119.3(6)
$S_{12}C_8C_3$				120.76	120.84	120.97	120.74	120.82	120.88	119.9(6)−119.7(6)
$C_3C_8C_9$				129.51	129.08	128.26	129.50	129.13	128.39	129.4(7)−129.7(7)
$C_8S_{12}C_{11}$				91.61	91.77	91.55	92.00	92.13	91.88	91.9(3)−91.8(4)
$C_8C_9C_{10}$				113.89	113.59	113.18	114.17	113.83	113.31	113.7(7)−114.0(7)
$C_{17}C_{18}C_{19}$							113.11	112.62	112.91	113.1(8)−113.6(8)
$S_{16}C_{15}C_{11}$							120.76	120.84	120.97	120.9(6)−121.1(6)
$S_{12}C_{11}C_{15}$							120.65	120.67	120.83	121.0(6)−121.4(6)
$C_{15}S_{16}C_{17}$							91.60	91.76	91.55	91.2(4)−91.6(4)
$H_6C_5C_1$	122.57	122.71	123.26	122.64	122.81	123.37	122.56	122.81	123.37	
$H_7C_4C_3$	123.32	123.42	123.78	122.62	122.76	123.35	122.59	122.80	123.37	
$H_{13}C_9C_8$				122.62	122.78	123.31	122.64	122.82	123.38	
$H_{14}C_{10}C_{11}$				123.29	123.41	123.78	122.59	122.75	123.35	
$H_{20}C_{19}C_{15}$							122.65	122.77	123.30	
$H_{21}C_{18}C_{17}$							123.29	123.41	123.78	
$H_xC_yC_z$[c]	126.75	128.46	127.87	128.77	128.49	127.87	128.76	128.47	127.87	
$S_2C_1C_{1'}S_{2'}$[e]	−17.57	−22.56	−32.67	−0.06	−14.46	−29.79	−0.14	−9.45	−29.68	
$S_2C_3C_8S_{12}$[e]				0.10	17.43	31.29	1.01	12.26	29.81	
$S_{12}C_{11}C_{15}S_{16}$[e]							−2.44	−18.34	−31.21	
$C_1S_2C_3C_4$	0.64	0.74	0.71	0.00	−1.22	−1.43	−0.05	−0.96	−1.47	
$S_2C_3C_4C_5$	−0.53	−0.62	−0.58	0.00	0.90	1.07	0.03	0.68	1.11	
$C_1S_2C_3C_8$				179.99	179.14	178.95	179.98	179.19	178.94	
$C_3C_4C_5C_1$	0.08	0.10	0.06	0.00	0.04	−0.02	0.00	0.08	0.00	
$C_8C_9C_{10}C_{11}$				0.00	0.05	0.05	0.00	0.00	0.00	
$C_8S_{12}C_{11}C_{10}$				0.00	0.61	0.71	0.16	1.23	1.44	
$C_9C_8S_{12}C_{11}$				0.00	0.57	0.67	0.18	−1.23	−1.44	
$C_{15}C_{19}C_{18}C_{17}$							0.00	−0.09	−0.03	
$C_{19}C_{15}S_{16}C_{17}$							0.09	0.52	0.69	
$C_{15}C_{11}S_{12}C_8$							180.12	181.00	181.01	
$C_{18}C_{19}C_{15}C_{11}$							179.99	179.83	179.71	
$H_6C_5C_1S_2$	179.20	179.12	180.73	180.00	180.66	179.31	180.01	180.49	180.66	
$H_7C_4C_3S_2$	180.01	179.97	180.09	179.99	179.28	179.37	179.94	179.38	179.35	
$H_{13}C_9C_8S_{12}$				179.99	179.19	179.21	179.94	179.32	179.33	
$H_{14}C_{10}C_{11}S_{12}$				179.99	180.00	179.94	180.12	180.79	180.62	
$H_{20}C_{19}C_{15}S_{16}$							180.15	180.93	180.75	
$H_{21}C_{18}C_{17}S_{16}$							179.99	179.96	180.10	
$H_xC_yC_zC_w$[d]	179.40	179.42	179.64	179.99	179.57	180.35	180.09	180.46	180.30	

[a] For comparison, the experimental bond length (Å) and angles (deg) of α-6T (ref 18) are also reported, along with the estimated error on the last digit within parentheses. Since in ref 18 no symmetry restrictions were applied, both estimated values are reported in case the bond lengths and angles coincide in C_2 symmetry. [b] H_xC_y: C_3H_8 for α-2T; $C_{11}H_{15}$ for α-4T; $C_{17}H_{22}$ for α-6T. [c] $H_xC_yC_z$: $H_8C_3C_4$ for α-2T; $H_{15}C_{11}C_{10}$ for α-4T; $H_{22}C_{17}C_{18}$ for α-6T. d$H_xC_yC_zC_w$: $H_8C_3C_4C_5$ for α-2T; $H_{15}C_{11}C_{10}C_9$ for α-4T; $H_{22}C_{17}C_{18}C_{19}$ for α-6T. eThe angle reported is α while the actual angle is (180°−α).

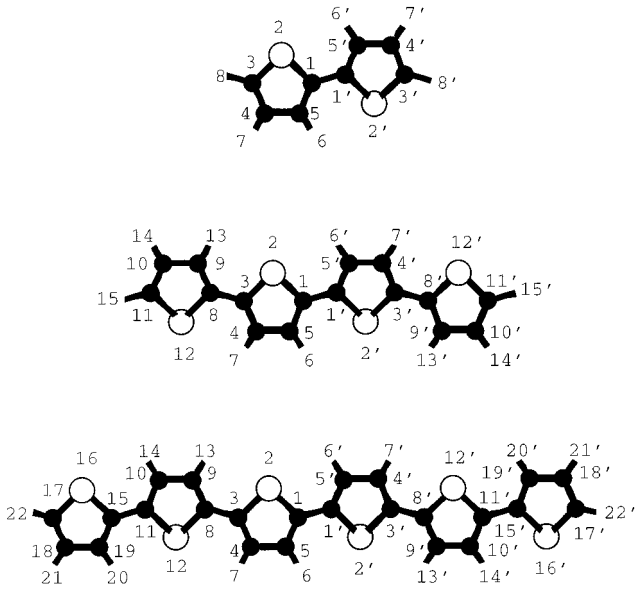

Figure 1. Atom labeling of the three oligomers of thiophene.

the 6-31G* basis set[9] in the previous study. We therefore used this basis set throughout the work. Two different models were used. They are energy functionals derived within the context of the density functional theory (DFT) and are usually referred to by acronyms, namely BLYP[6] and B3LYP.[7] Following the Gaussian notation,[8] the functionals are written in the general form

$$a_1E(\mathrm{S})_x + a_2E(\mathrm{HF})_x + a_3E(\mathrm{B88})_x + a_4E(\mathrm{local})_c + a_5E(\mathrm{nonlocal})_c \quad (1)$$

where $E(\mathrm{S})_x$ is the Slater exchange functional,[10] $E(\mathrm{HF})_x$ is the Hartree−Fock exchange, $E(\mathrm{B88})_x$ is the nonlocal exchange functional proposed by Becke in 1988,[11] $E(\mathrm{local})_c$ is a local correlation functional, in this case the Vosko, Wilk, Nusair functional,[13] and $E(\mathrm{nonlocal})_x$ is the Lee−Yang−Parr correlation functional[12] that includes both local and nonlocal terms. In the BLYP model, $a_1 = a_3 = a_5 = 1$ and $a_2 = a_4 = 0$; in the B3LYP model, $a_1 = 0.80$, $a_2 = 0.20$, $a_3 = 0.72$, $a_4 = 0.19$, and $a_5 = 0.81$.

The Gaussian package calculates directly the infrared intensities but does not perform the calculation of the inelastic neutron scattering cross sections which were obtained by the CLIMAX program[14] that had been modified in our previous work[5] to use and scale *ab initio* force constants.

Interestingly, the DFT simulations required less use of the experimental data than the Hartree−Fock (HF) ones. The lattice mode spectrum[16] and the phonon wings were obtained extracting only 120−140 cm^{-1} of the experimental spectrum (it was 160−180 cm^{-1} before). Two more quantities that were different in the DFT simulations were the damping parameter[5] of the Debye−Waller factor[17] that was reduced from 0.3 to 0.2 and the external Debye−Waller factor, which also entered in the definition of the phonon wings intensities, that was set to 9.0 $\times 10^3$ (it was 8.0 $\times 10^3$ in the HF calculations).

In principle, one would also be interested in testing the Raman scattering cross sections. Unfortunately, the DFT derivatives of the polarizability tensor are not yet available, and we had to forfeit this part of the study.

3. Results and Discussion

A. The Optimized Structural Parameters. The prerequisite for the discussion of the simulation of the response to infrared photons and slow neutrons is the exam of the structural parameters—bond lengths and bond angles—obtained by geometry optimization. Two different trends are assessed here. They are the variation of selected parameters with the elongation

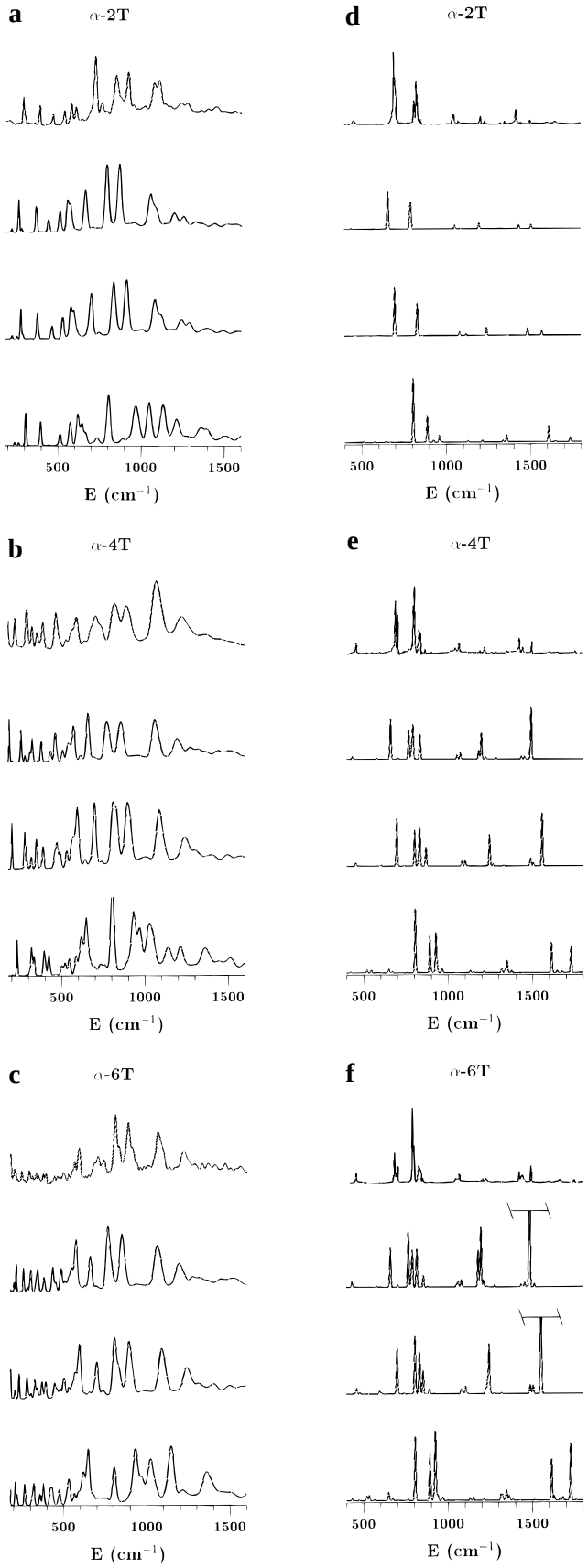

Figure 2. Comparison of experiments and calculations. From top to bottom: experimental, BLYP/6-31G*, B3LYP/6-31G*, and HF/6-31G* spectra; (a) INS spectrum of α-2T, (b) INS spectrum of α-4T, (c) INS spectrum of α-6T, (d) infrared spectrum of α-2T, (e) infrared spectrum of α-4T, (f) infrared spectrum of α-6T.

TABLE 2: Comparison of Experiments and Calculations for α-2T: (a) Experimental Frequencies and, in Parentheses, the Source of the Experimental Data, (b) Calculated Frequencies, (c) Difference between Experimental and Calculated Frequencies, (d) Calculated Infrared Intensities (km/mol), (e) Calculated INS Intensities, (f) Scaled Frequencies, and (g) Difference between Experimental and Scaled Frequencies

			BLYP				B3LYP				BLYP		B3LYP	
no.	a		b	c	d	e	b	c	d	e	f	g	f	g
1	3104	(R)	3185.6	−81.6	0.0	0.8	3270.7	−166.7	0.0	1.0	3116.2	−12.2	3115.6	−11.7
2	3071	(R)	3144.1	−73.1	0.3	4.2	3231.6	−160.6	0.3	4.6	3075.1	−4.1	3078.2	−7.2
3	3060	(R)	3129.9	−69.9	0.0	4.0	3217.2	−157.2	0.0	4.3	3061.2	−1.2	3064.5	−4.5
4	1553	(R)	1545.7	7.3	0.0	3.9	1612.2	−59.2	0.1	3.7	1549.6	3.4	1545.7	7.3
5	1441	(R,ir)	1446.0	−5.0	0.3	3.0	1503.8	−62.8	0.6	2.9	1447.2	−6.2	1445.0	−4.0
6	1367	(R,ir)	1368.9	−1.9	0.0	3.1	1413.2	−46.2	0.0	3.1	1362.7	4.3	1369.7	−2.7
7	1248	(R,ir)	1251.7	−3.7	0.0	10.2	1288.9	−40.9	0.0	10.7	1253.6	−5.6	1251.1	−3.1
8			1189.0		0.8	2.5	1240.9		1.6	1.6	1206.6		1208.7	
9	1078	(R)	1080.6	−2.6	0.0	6.4	1114.2	−36.2	0.0	6.7	1081.3	−3.3	1080.7	−2.7
10	1050	(R)	1048.9	1.1	0.1	13.9	1077.2	−27.2	0.1	14.5	1036.0	14.0	1039.3	10.7
11	916	(n)	864.2	51.8	0.2	15.6	909.3	6.7	0.4	15.7	903.1	12.9	909.3	6.7
12	856	(R,ir)	829.1	26.9	0.5	2.7	862.7	−6.7	1.0	2.7	860.6	−4.6	861.4	−5.4
13	816	(ir,*)	786.5	29.5	28.1	15.8	827.4	−11.4	24.8	16.0	821.8	−5.8	827.4	−11.4
14	741	(R,n)	707.0	34.0	0.0	0.4	742.4	−1.4	0.1	0.6	735.0	6.0	741.3	−0.3
15	695	(ir)	657.3	37.7	78.3	7.0	695.8	−0.8	109.5	9.2	686.2	8.8	695.7	−0.7
16	674	(R)	653.3	20.7	16.7	2.9	681.5	−7.5	0.4	2.4	673.5	0.5	674.9	−0.9
17	574	(n)	553.4	20.6	0.6	9.8	574.8	−0.8	0.3	10.3	578.3	−4.3	574.8	−0.8
18	464	(n,ir)	440.2	23.8	2.4	3.2	463.1	0.9	2.6	3.3	459.6	4.4	462.9	1.1
19	383	(n)	366.5	16.5	0.1	5.2	375.6	7.4	0.1	5.2	376.8	6.2	372.0	11.0
20	286	(n,R)	278.6	7.3	0.0	0.6	289.2	−3.2	0.0	0.7	288.0	−2.0	286.6	−0.6
21			109.7		1.3	4.9	112.4		1.5	5.0	114.7		112.4	
22			25.2		0.4	8.5	32.8		0.4	8.3	26.3		32.8	
23	3104	(ir)	3185.7	−81.7	1.4	0.8	3270.7	−166.7	1.1	1.0	3116.2	−12.2	3115.6	−11.6
24	3075	(ir)	3143.8	−68.8	14.1	4.2	3231.3	−156.3	10.2	4.6	3074.8	0.2	3077.9	−2.9
25	3063	(ir)	3130.2	−67.2	23.4	4.0	3217.5	−154.5	20.4	4.3	3061.4	1.6	3064.7	−1.7
26	1498	(ir)	1506.2	−8.2	11.2	5.9	1568.6	−70.6	11.0	5.6	1510.6	−12.6	1507.9	−9.9
27	1416	(ir)	1433.0	−17.0	10.5	2.8	1483.0	−67.0	16.3	2.9	1424.3	−8.3	1425.4	−9.4
28	1323	(ir)	1322.7	0.3	1.5	2.9	1370.5	−47.5	0.9	2.9	1320.6	2.4	1324.0	−1.0
29	1208	(ir)	1197.9	10.1	14.5	10.0	1240.2	−32.2	17.0	10.4	1197.9	10.1	1199.7	8.3
30	1078	(ir)	1087.7	−9.7	2.5	9.1	1119.1	−41.1	3.6	8.6	1087.7	−9.7	1085.0	−7.0
31	1050	(ir)	1054.2	−4.2	9.4	12.0	1081.7	−31.7	8.4	13.1	1038.0	12.0	1041.8	8.2
32	916	(ir)	867.7	48.3	0.2	9.1	911.5	4.5	0.0	15.3	905.4	10.6	911.5	4.5
33			865.0		0.3	12.2	901.3		0.8	2.7	899.2		900.3	
34		(*)	794.2		26.1	10.2	838.7		3.0	14.2	829.5		838.7	
35	827	(ir,*)	791.3	35.7	32.3	10.0	830.5	−3.5	56.2	4.1	826.1	0.9	830.2	−3.2
36	741	(n,*)	702.3	38.7	0.1	0.6	740.6	0.4	0.0	0.6	730.8	10.2	739.7	1.3
37	705	(ir)	666.0	39.0	2.4	9.1	701.0	4.0	3.9	10.2	696.0	9.0	701.0	4.0
38			585.0		1.2	1.3	610.7		1.3	2.0	606.2		610.1	
39	601	(n)	571.2	29.8	0.7	8.5	593.9	7.1	1.1	8.9	596.3	4.7	593.8	7.2
40	532	(n)	507.9	24.1	0.7	6.4	527.6	4.4	1.1	6.7	530.7	1.3	527.6	4.4
41	286	(n)	261.2	24.8	0.0	4.5	276.4	9.6	0.0	4.5	272.8	13.2	276.4	9.6
42			127.4		0.2	5.1	127.1		0.2	5.1	131.9		127.2	

of the chain and their further variation as a function of the model. The parameters that we have selected for discussion are (i) the $C_\alpha-C_\alpha$, $C_\alpha-C_\beta$, $C_\beta-C_\beta$ and C−S bond lengths and the S-$C_\alpha-C_\alpha$−S torsional angle of the central bithiophene unit (see Table 1) and (ii) the variation of the same parameters along the chain of α-6T.

The atomic numbering is the same we adopted in our previous work and can be found in Figure 1. Readers interested in other bond distances or bond angles are referred to Table 1.

BLYP/6-31G*, B3LYP/6-31G*, and HF/6-31G* concur that, in the central fragment, $C_\alpha-C_\alpha$ and $C_\beta-C_\beta$ decrease upon chain elongation, while the C−S and $C_\alpha-C_\beta$ increase slightly. Similarly, the central S−$C_\alpha-C_\alpha$−S angle decreases going from α-2T to α-4T to α-6T. In α-6T the opposite trend is observed as one moves from center to chain ends (increase of $C_\alpha-C_\alpha$ and $C_\beta-C_\beta$ and decrease of C−S and $C_\alpha-C_\beta$).

When considering the three models, one expects BLYP/6-31G* to account best for electron correlation and HF/6-31G* to be the least correlated. In this sense, for $C_\alpha-C_\alpha$, correlation decreases the bond lengths, while it increases the C−S and $C_\alpha-C_\beta$ ones. The S−$C_\alpha-C_\alpha$−S angles are also decreased by electron correlation. It may therefore be argued that the correlation effect is quite similar to the effect of chain elongation on the central unit.

In these systems, correlation can act in two major ways: the first is by modifying the sulfur−hydrogen nonbonding interaction, the second is through the π-electron delocalization. From the results reported above, it appears that electron correlation decreases the H···S interaction and/or requires the maximization of the overlap of the π-electron system.

Inspection of the other degrees of freedom did not show major or regular differences that can be ascribed to the material in a systematic way. Interestingly, however, if one assesses the bond distances and bond angles obtained by the three models in light of the experimental structure of α-6T,[18] the best agreement is found for the Hartree−Fock/6-31G* calculations while BLYP/6-31G* gives the worst agreement with a tendency to overestimate all the bond distances. In particular, all the BLYP/6-31G* C−S bond lengths appear to be about 0.05 Å longer than the experimental ones.

In passing, we note that some of the inconsistencies of Table 1 of ref 5 are corrected in the present Table 1.

B. The Infrared and Inelastic Neutron Scattering Spectra. One of the purposes of the present work is to assess the performance of two density functionals in the simulation of vibrational spectra. Of the several techniques one can use to probe the vibrational states, infrared is the most common. In this kind of experiment, apart from the frequency, the intensity

TABLE 3: Comparison of Experiments and Calculations for α-4T: (a) Experimental Frequencies and, in Parentheses, the Source of the Experimental Data, (b) Calculated Frequencies, (c) Difference between Experimental and Calculated Frequencies, (d) Calculated Infrared Intensities (km/mol), (e) Calculated INS Intensities, (f) Scaled Frequencies, and (g) Difference between Experimental and Scaled Frequencies

			BLYP				B3LYP				BLYP		B3LYP	
no.	a		b	c	d	e	b	c	d	e	f	g	f	g
1	3109	(R)	3186.4	−77.4	0.0	6.2	3271.5	−162.5	0.0	5.8	3110.6	−1.6	3116.4	−7.4
2	3102	(R)	3143.5	−41.5	0.0	2.0	3231.6	−129.6	0.2	1.8	3068.2	33.8	3078.2	23.8
3	3071	(R)	3141.8	−70.8	0.0	2.3	3230.0	−159.0	0.1	2.5	3066.5	4.5	3076.7	−5.7
4			3129.2		0.0	1.8	3217.3		0.1	1.8	3054.3		3064.5	
5	3060	(R)	3127.3	−67.3	0.0	2.2	3215.8	−155.8	0.0	2.5	3052.4	7.6	3063.1	−3.1
6	1560	(R)	1551.0	9.0	0.0	2.3	1619.6	−59.6	0.0	2.2	1553.7	6.3	1552.3	7.7
7	1515	(R)	1510.7	4.3	0.0	3.0	1576.8	−61.8	0.0	2.6	1513.5	1.5	1514.1	0.9
8	1460	(R)	1442.2	17.8	0.0	1.9	1507.4	−47.4	0.4	1.6	1443.4	16.6	1448.8	11.2
9	1427	(R)	1435.4	−8.4	0.0	1.4	1489.0	−62.0	0.3	1.6	1429.5	−2.5	1431.3	−4.3
10	1365	(R)	1377.2	−12.2	0.0	1.9	1416.1	−51.1	0.0	1.9	1366.4	−1.4	1371.7	−6.7
11			1330.5		0.0	3.0	1373.3		0.0	2.6	1329.7		1329.5	
12			1266.5		0.0	6.5	1300.1		0.0	6.8	1271.2		1261.5	
13	1220	(R)	1210.4	9.6	0.0	4.5	1255.2	−35.2	0.0	3.1	1221.4	−1.4	1224.4	−4.4
14			1195.4		0.0	1.7	1244.7		1.8	2.6	1211.6		1207.4	
15			1187.9		0.0	4.1	1235.3		0.6	4.9	1194.6		1197.8	
16	1085	(R)	1085.5	0.5	0.0	4.0	1117.4	−32.4	0.0	3.0	1085.2	−0.2	1083.3	1.7
17	1055	(R)	1061.0	−6.0	0.0	8.1	1087.7	−32.7	0.1	9.6	1052.9	2.1	1052.5	2.5
18	1049	(R)	1050.5	−1.5	0.0	9.2	1078.3	−29.3	0.4	9.3	1038.5	10.5	1041.6	7.4
19			864.3		0.0	6.5	910.3		0.2	6.2	911.9		910.3	
20	890	(n,*)	859.6	30.4	0.0	2.1	895.1	−5.1	0.3	3.2	890.6	−0.6	893.5	−3.5
21	878	(R)	844.2	33.8	0.1	5.8	887.8	−9.8	0.0	8.8	889.8	−11.8	887.6	−9.6
22	839	(R,*)	807.1	31.9	0.0	2.7	843.4	−4.4	1.2	2.7	843.6	−4.6	842.4	−3.4
23	821	(ir,*)	782.2	36.8	24.5	5.9	828.8	−7.8	14.6	7.7	825.2	−4.2	828.7	−7.7
24	794	(ir)	765.8	28.2	69.5	6.9	805.8	−11.8	80.8	10.6	807.9	−13.9	805.8	−11.8
25	740	(n,*)	704.9	35.1	0.0	0.2	741.0	−1.0	0.0	0.3	735.0	5.0	740.0	0.0
26			695.3		0.0	0.4	734.2		0.0	0.5	724.5		732.8	
27	803	(ir,*)	670.2	32.8	0.0	0.4	701.4	1.6	16.3	2.4	689.2	13.8	697.8	5.2
28	688	(ir,*)	659.0	29.0	93.9	8.9	697.1	−9.1	91.9	8.8	688.6	−0.6	692.6	−4.6
29	639	(n,R)	613.8	25.2	0.0	1.8	640.2	−1.2	0.2	1.9	631.6	7.4	635.4	3.6
30	596	(n,R)	573.0	23.0	1.7	4.5	595.1	0.9	1.2	6.0	604.5	−8.5	595.0	1.0
31			549.0		0.1	4.7	572.1		0.0	6.3	579.2		572.1	
32	529	(n,R)	507.7	21.3	0.1	3.3	530.9	−1.9	0.2	4.1	535.6	−6.6	530.8	−1.8
33	471	(n,R)	460.9	10.1	0.0	5.5	473.1	−2.1	0.7	5.7	468.7	2.3	465.8	5.2
34	456	(n,R,ir)	433.9	22.1	7.3	2.6	459.6	−3.6	7.4	3.2	457.8	−1.8	458.3	−2.3
35	369	(R)	359.4	9.6	0.0	0.2	373.4	−4.4	0.0	0.3	372.4	−3.4	371.6	−2.6
36	320	(n,R)	311.7	8.3	0.0	1.7	318.4	1.6	0.1	1.8	319.8	0.2	316.8	3.2
37	290	(n,R)	257.8	32.2	0.3	4.3	279.0	11.0	0.4	4.7	272.0	18.0	279.0	11.0
38			154.2		0.0	1.5	159.7		0.0	1.7	158.8		115.7	
39			132.9		0.6	4.6	135.8		0.7	4.8	140.2		135.8	
40			102.0		0.0	3.4	99.6		0.0	3.4	105.0		99.6	
41			32.6		1.5	4.3	44.0		2.0	6.7	34.4		44.0	
42			18.1		0.0	8.2	19.7		0.1	5.1	19.1		19.7	
43			3.2		0.8	7.6	15.4		0.0	8.0	3.4		15.4	
44	3110	(ir)	3186.4	−76.4	0.8	6.2	3271.5	−161.5	1.1	5.8	3110.6	−0.6	3116.4	−6.4
45	3100	(ir)	3143.5	−43.5	19.9	2.0	3231.5	−131.5	13.6	1.8	3068.2	31.8	3078.2	21.8
46	3079	(ir)	3141.7	−62.7	6.5	2.2	3230.0	−151.0	4.0	2.5	3066.5	12.5	3076.7	2.3
47	3062	(ir)	3129.2	−67.2	37.9	1.8	3217.2	−155.2	31.4	1.8	3054.2	7.8	3064.5	−2.5
48	3046	(ir)	3127.3	−81.3	42.9	2.2	3215.8	−169.8	43.8	2.5	3052.4	−6.4	3063.2	−17.2
49			1534.6		0.3	2.4	1603.0		0.4	2.2	1537.8		1537.6	
50	1494	(ir)	1491.9	2.1	121.5	3.9	1556.9	−62.9	100.9	3.6	1495.4	−1.4	1497.3	−3.3
51	1449	(ir)	1454.7	−5.7	7.8	1.9	1505.8	−56.8	7.3	2.1	1448.3	0.7	1449.5	−0.5
52	1425	(ir)	1435.4	−10.4	8.3	1.8	1488.4	−63.4	20.2	1.5	1428.6	−3.6	1430.4	−5.4
53	1355	(ir)	1361.0	−6.0	0.5	2.2	1403.6	−48.6	0.1	1.9	1354.3	0.7	1358.5	−3.5
54	1290	(ir)	1287.1	2.9	3.6	3.5	1330.2	−40.2	2.1	3.1	1284.8	5.2	1283.2	6.8
55	1220	(ir)	1223.1	−3.1	6.0	4.8	1264.6	−44.6	4.0	5.0	1227.2	−7.2	1222.3	−2.3
56			1196.9		61.0	4.3	1243.9		69.7	2.8	1205.5		1209.5	
57	1195	(ir)	1181.7	13.3	22.1	5.3	1226.4	−31.4	0.2	6.8	1186.6	8.4	1187.6	7.4
58	1085	(ir)	1087.0	−2.0	0.0	5.3	1117.7	−32.7	1.7	3.3	1085.4	−0.4	1083.5	1.5
59	1067	(ir)	1073.3	−6.3	15.7	8.1	1099.1	−32.1	12.3	10.3	1065.5	1.5	1064.2	2.8
60	1046	(ir)	1053.9	−7.9	10.2	7.9	1080.6	−34.6	9.7	8.0	1038.8	7.2	1042.1	3.9
61	920	(n)	877.6	42.4	0.3	1.8	914.3	5.7	0.3	2.9	911.9	8.1	912.8	7.2
62			864.4		0.0	6.5	909.9		0.2	6.1	909.1		909.7	
63	890	(n)	848.2	41.8	0.0	5.7	893.0	−3.0	0.3	8.8	894.8	−4.8	892.9	−2.9
64	862	(ir)	833.0	29.0	58.5	2.5	868.1	−6.1	38.3	2.7	866.7	−4.7	866.8	−4.8
65	835	(ir,*)	790.9	44.1	79.6	2.3	832.1	2.9	58.7	4.2	832.0	3.0	831.8	3.2
66	827	(ir,*)	782.2	44.8	0.0	5.9	828.3	−1.3	21.8	6.8	825.2	1.8	828.2	−1.2
67	798	(ir)	763.9	34.1	0.0	6.7	807.1	−9.1	0.9	10.3	805.9	−7.9	807.1	−9.1
68	740	(n,*)	703.3	36.7	3.0	0.3	740.4	−0.4	1.5	0.3	734.3	5.7	739.5	0.5
69			691.2		0.4	0.3	732.2		0.2	0.4	722.1		731.3	
70	692	(R,n,*)	659.1	32.9	0.0	8.9	697.6	−5.6	2.9	9.5	695.4	−3.4	697.6	−5.6
71			649.1		0.1	1.1	677.6		0.3	1.2	666.5		670.3	
72			578.6		2.9	0.4	607.3		2.2	1.5	608.1		606.6	

TABLE 3: (Continued)

			BLYP				B3LYP				BLYP		B3LYP	
no.	a		b	c	d	e	b	c	d	e	f	g	f	g
73	590	(n)	576.4	13.6	0.0	4.4	596.9	−6.9	2.6	6.3	597.8	−7.8	596.9	−6.9
74			566.6		0.0	4.3	587.8		0.4	5.4	595.9		587.8	
75	560	(n)	535.4	24.6	0.0	4.0	558.1	1.9	0.1	5.0	564.9	−4.9	558.1	1.9
76	500	(n)	467.5	32.5	0.0	3.0	491.4	8.6	3.4	3.5	493.2	6.8	491.4	8.6
77	388	(n)	379.0	9.0	1.5	4.0	388.7	−0.7	1.5	4.1	387.3	0.7	385.1	2.9
78	353	(n)	325.2	27.8	0.0	3.9	349.3	3.7	0.0	4.8	343.1	9.9	349.1	3.9
79	290	(n)	282.3	7.7	4.5	1.0	291.8	−1.8	3.5	1.1	291.6	−1.6	289.0	1.0
80	220	(n)	188.2	31.8	0.0	4.2	203.3	16.7	0.0	4.3	198.5	21.5	203.2	16.8
81			164.4		0.2	4.2	161.6		0.1	4.2	169.1		161.6	
82			70.0		0.0	3.0	73.0		0.0	3.0	73.9		73.0	
83			42.5		0.1	1.8	40.7		0.1	1.9	43.7		40.7	
84			11.7		0.0	8.7	27.6		0.0	8.3	12.3		27.6	

of the response depends on the shape of the vibrational motion and the dipole moment surface. A less common experimental approach is to use inelastic neutron scattering. In this kind of experiment, a slow neutron gains energy from the impact and subsequent inelastic scattering from the sample. In the crudest model, the response of the system can be described as due to the product of a temperature factor, or Debye−Waller factor, which can be taken to be proportional to the mean square motion of the atoms and another factor that describes the dynamics of the vibrational motion (more quantitative details can be found in ref 5). The response is therefore due to the shape of the modes only. From the theoretical point of view, simulation of the inelastic neutron scattering spectrum should precede simulation of the infrared spectrum which requires more data. Experimentally, the situation is reversed because of the wide availability of infrared equipment and the small abundance of neutron sources dedicated to vibrational work. Perhaps not too surprisingly, a similar situation occurs also in quantum chemistry where most quantum chemical packages can simulate infrared spectra and none−to the best of our knowledge−can simulate inelastic neutron scattering spectra. The simulation of the INS spectra was performed by the CLIMAX package[14] that had been suitably modified to handle the refinement of *ab initio* force fields.[5]

In Figure 2, we show the comparison between experimental and calculated spectra. It is important to emphasize the good agreement obtained for the INS spectra by the DFT methods. If a criticism must be voiced, at all, this is the slight overestimate of the intensity of the doublet in the region between 750−950 cm^{-1}. Minor adjustments in the content of CCH bendings can improve the situation. It is important to mention, however, that the discrepancy may also arise from the treatment of the Debye−Waller factor, a parameter that we treat empirically. The agreement obtained by the DFT models is superior to that obtained by the Hartree−Fock calculations. The quality of the DFT simulations must be taken to indicate that the shape of the vibrational modes is calculated accurately.

The neutron spectra are intrinsically broad. The broadening is due to a number of factors that can be summarized as due to (a) a failure of the isolated molecule model that does not include lattice phonons, i.e. the intermolecular vibrations, and the external Debye−Waller effect, (b) anharmonicity effects that make the fundamentals interact with the density of vibrational states, (c) instrumental resolution. Reassuringly, the quantities involved in the DFT simulations are on average smaller than the corresponding ones used for the HF spectra.

The DFT simulation of the infrared spectra is somewhat less satisfactory because of the presence of an excess of intensity in modes that are silent or nearly silent experimentally. In particular, one can notice that the agreement worsens with the increase of the molecular size. Owing to and only because of the present INS simulation, it is now possible to ascribe this defect to the surface of the dipole moment. Visualization of the most intense modes carrying the spurious intensity diplayed in-phase motion of all the hydrogen atoms. Although not fully understood at this stage, the presence of a factor common to all these vibrations makes us believe that we may have encountered a systematic shortcoming of the computational theory. Were a similar effect present in other extended systems, it would certainly be worthy of investigation in the future. In any event, the silver lining in the cloud is that all the intense modes are consistently present in the spectra. As a consequence, if a band is calculated by these methods to have little intensity, it ought to be absent from the spectrum.

In Tables 2, 3, and 4, the details of the experimental and calculated frequencies are presented. The tables supersede the assignments reported in the previous work. The frequencies that have been reassigned are labeled with an asterisk. In general, the reassigments pertain to bands that fall within a few cm^{-1} and have been introduced with the only aim of improving the standard deviation of the fitting. With the present assignment the overall standard deviations between the experimental and the calculated frequencies are 35.3 cm^{-1} at the BLYP/6-31G* level and 69.4 cm^{-1} at the B3LYP/6-31G* level. The same deviations for the individual molecules are 38.4 and 77.0 cm^{-1} for α-2T, 34.5 and 68.1 cm^{-1} for α-4T, and 34.8 and 67.4 cm^{-1} for α-6T. Apart from these values, it is interesting to note some trends that are shared by the three molecules.

In the BLYP/6-31G* calculations one can observe the following:

(i) There is an overestimate of the CH stretching frequencies by about 80 cm^{-1}. Notice that because of the anharmonicity of the CH stretches, the "experimental" harmonic frequency is actually quite closer to the calculated value.

(ii) The region that starts around 1600 cm^{-1} and goes down to 1000 cm^{-1} is simulated with just a few cm^{-1} of difference. This is a remarkable achievement if one considers the inevitable presence of anharmonicities and Fermi resonances that are not included in the calculations.

(iii) Below 1000 cm^{-1}, differences up to 50 cm^{-1} are found. They tend to taper off with the decrease of the energy of the vibrational quantum, although they remain of the order of 10%.

Somewhat different trends are found in the B3LYP/6-31G* calculations. Inspection shows that (i) they overestimate the CH stretching frequencies by up to 160 cm^{-1}, (ii) in the region that starts around 1600 cm^{-1} and goes down to 1000 cm^{-1} they show differences of up to 70 cm^{-1}, (iii) below 1000 cm^{-1} they give a very nice agreement with the experiment.

It therefore appears that the two methods are complementary. BLYP/6-31G* is better suited to treat the region above 1000 cm^{-1} while B3LYP/6-31G* can become the method of choice to treat the region below 1000 cm^{-1}.

The frequency reassignments of Tables 2, 3, and 4 are possible because of the smaller uncertainty in matching experi-

TABLE 4: Comparison of Experiments and Calculations for α-6T: (a) Experimental Frequencies and, in Parentheses, the Source of the Experimental Data, (b) Calculated Frequencies, (c) Difference between Experimental and Calculated Frequencies, (d) Calculated Infrared Intensities (km/mol), (e) Calculated INS Intensities, (f) Scaled Frequencies, and (g) Difference between Experimental and Scaled Frequencies

			BLYP				B3LYP				BLYP		B3LYP	
no.	a		b	c	d	e	b	c	d	e	f	g	f	g
1	3110	(R)	3186.4	−76.4	0.0	6.1	3271.4	−161.4	0.0	5.9	3116.9	−6.9	3116.1	−6.1
2	3102	(R)	3144.0	−42.0	0.0	2.0	3231.9	−129.9	0.2	2.3	3074.9	27.1	3078.5	23.5
3	3088	(R)	3142.5	−54.5	0.0	2.9	3230.1	−142.1	0.1	3.1	3073.6	14.4	3076.8	11.2
4			3142.2		0.0	2.7	3229.8		0.0	3.2	3073.2		3076.5	
5	3070	(R)	3129.8	−59.8	0.0	1.9	3217.8	−147.8	0.2	1.8	3061.1	8.9	3065.1	4.9
6	3054	(R)	3128.0	−74.0	0.0	2.8	3215.8	−161.8	0.1	3.5	3059.3	−5.3	3063.2	−9.2
7	3048	(R)	3127.7	−79.7	0.0	2.7	3215.5	−167.5	0.0	3.2	3059.1	−11.1	3062.8	−14.8
8	1564	(R)	1551.4	12.6	0.0	2.7	1620.3	−56.3	0.0	2.6	1554.7	9.3	1553.0	11.0
9	1542	(R)	1530.8	11.2	0.0	2.8	1599.2	−57.2	0.0	2.6	1534.6	7.4	1533.9	8.1
10	1504	(R)	1498.5	5.5	0.0	4.0	1564.2	−60.2	0.2	3.8	1502.3	1.7	1503.4	0.6
11	1458	(R)	1453.4	4.6	0.0	2.3	1506.0	−48.0	0.2	2.1	1447.9	10.1	1449.3	8.7
12			1435.9		0.0	1.8	1494.2		0.3	1.7	1430.2		1435.8	
13	1430	(R)	1422.3	7.7	0.0	1.8	1488.2	−58.2	0.3	2.0	1428.4	1.6	1430.2	−0.2
14	1368	(R)	1381.0	−13.0	0.0	2.4	1418.4	−50.4	0.0	2.6	1370.1	−2.1	1373.6	−5.6
15			1355.9		0.0	3.1	1397.5		0.0	3.4	1351.8		1352.5	
16			1307.6		0.0	5.3	1348.1		0.0	4.7	1311.4		1305.1	
17			1271.2		0.0	7.4	1305.3		0.0	8.0	1275.3		1265.1	
18			1220.4		0.0	5.4	1263.9		0.1	4.6	1227.4		1228.2	
19	1219	(R,*)	1204.7	14.3	0.0	4.8	1251.1	0.0	0.1	3.2	1215.8	3.2	1215.3	3.7
20			1196.3		0.0	2.5	1247.1	−28.1	0.7	4.8	1212.1		1208.5	
21			1192.4		0.0	4.0	1241.4		2.4	3.8	1201.5		1201.2	
22			1181.3		0.0	5.9	1228.2		0.0	7.1	1185.9		1189.9	
23			1086.3		0.0	4.9	1117.7		0.0	3.7	1085.3		1083.2	
24			1072.0		0.0	10.2	1098.3		0.0	11.7	1064.2		1062.6	
25	1050	(R,*)	1056.6	−6.6	0.0	9.6	1084.2	−34.2	0.1	10.8	1049.8	0.2	1050.4	−0.4
26			1050.0		0.0	11.2	1078.6	0.0	0.4	10.9	1039.8		1041.6	
27	911	(n)	870.9	40.1	0.0	2.1	910.9	0.1	0.2	6.2	903.6	7.4	910.6	0.4
28			864.7		0.0	7.0	907.0		0.1	3.5	902.7		900.3	0.0
29	885	(n)	847.7	37.3	0.1	9.3	891.9	−6.9	0.1	9.9	885.8	−0.8	891.4	−6.4
30			842.8		0.0	10.0	885.5		0.0	9.9	880.7		885.5	
31			835.9		0.0	2.6	871.8		0.8	3.0	867.6		866.4	
32	832	(n)	799.1	32.9	0.0	2.6	837.6	−5.6	1.7	3.2	832.5	−0.5	829.8	2.2
33	827	(ir)	782.5	44.5	23.8	8.0	829.7	−2.7	13.6	8.0	817.7	9.3	815.2	11.8
34	795	(ir,*)	765.7	29.3	130.9	11.1	806.0	−11.0	77.9	11.7	800.2	−5.2	806.0	−11.0
35	791	(ir)	762.8	28.2	2.0	11.2	802.6	−11.6	71.8	11.4	797.1	−6.1	802.6	−11.6
36	743	(n,*)	704.5	38.5	0.0	0.2	740.8	2.2	0.0	0.6	732.3	10.7	733.8	9.2
37			697.1		0.0	0.4	735.0		0.0	0.7	723.7		730.8	
38			690.8		0.0	0.4	732.1		0.0	0.5	718.2		716.0	
39	705	(n)	672.7	32.3	0.0	0.2	705.0	0.0	5.9	1.0	691.5	13.5	698.6	6.4
40	688	(ir,*)	659.5	28.5	94.0	9.3	698.3	−10.3	102.6	9.8	689.2	−1.2	695.6	−7.6
41		(*)	647.5		0.0	1.3	676.7		0.0	1.9	666.5		666.1	
42	631	(n)	598.3	32.7	0.0	1.9	625.3	5.7	0.1	1.9	617.5	13.5	619.3	11.7
43	592	(n)	576.0	16.0	0.7	6.3	596.6	−4.6	0.6	6.8	601.9	−9.9	596.6	−4.6
44			569.4		0.9	6.2	591.3		0.6	6.3	595.0		591.2	
45	565	(n,*)	548.6	16.4	0.0	6.5	571.2	−6.2	0.0	6.9	573.3	−8.3	571.1	−6.1
46		(*)	526.3		0.0	5.1	550.2		0.1	5.4	550.0		549.9	
47	500	(n,*)	486.8	13.2	0.0	6.5	506.6	−6.6	0.2	4.6	502.9	−2.9	505.6	−5.6
48			481.1		0.1	4.0	498.2		0.2	5.9	496.1		488.6	
49	460	(n,ir)	433.2	26.8	12.1	3.2	460.2	−0.2	13.5	3.2	452.6	7.4	460.0	0.0
50	391	(n,*)	382.6	8.4	0.0	4.4	392.7	−1.7	0.1	4.4	393.5	−2.5	389.7	1.3
51		(*)	372.5		0.0	0.5	387.2		0.1	1.3	385.9		384.7	
52	335	(n,*)	303.4	31.6	0.2	4.9	327.2	7.8	0.2	4.9	317.0	18.0	327.0	8.0
53	310	(n)	297.5	12.5	0.0	1.3	305.0	5.0	0.1	1.3	307.0	3.0	303.5	6.5
54	290	(n,*)	282.6	7.4	0.0	0.9	292.0	−2.0	0.0	1.0	291.8	−1.8	287.3	2.7
55	248	(n)	214.8	33.2	0.2	4.8	232.2	15.8	0.3	4.5	224.5	23.5	232.2	15.8
56			139.6		0.0	3.1	143.8		0.5	4.6	145.5		143.8	
57			139.2		0.4	4.5	137.6		0.0	2.8	144.3		137.4	
58			102.1		0.0	3.2	105.6		0.0	3.3	105.3		104.3	
59			60.3		0.5	2.4	64.4		0.7	2.3	63.1		64.4	
60			51.7		0.0	1.8	49.9		0.0	1.6	53.6		49.9	
61			29.3		2.3	8.0	38.7		2.8	8.0	30.6		38.7	
62			18.2		0.3	9.2	27.3		0.0	8.4	19.0		27.3	
63			14.1		0.5	7.7	8.9		0.0	6.4	14.7		8.9	
64			6.1		0.3	4.7	7.3		0.1	6.3	6.4		7.3	
65	3110	(ir)	3186.4	−76.4	0.9	6.1	3271.4	−161.4	1.2	5.9	3116.9	−6.9	3116.1	−6.1
66	3100	(ir)	3143.9	−43.9	25.1	2.0	3231.9	−131.9	15.0	2.3	3074.9	25.1	3078.5	21.5
67	3079	(ir)	3142.4	−63.4	5.0	2.9	3230.0	−151.0	4.8	3.1	3073.5	5.5	3076.7	2.3
68			3142.2		8.2	2.7	3229.7		3.2	3.2	3073.2		3076.4	
69	3062	(ir)	3129.7	−67.7	47.2	1.9	3217.8	−155.8	37.2	1.8	3061.0	1.0	3065.1	−3.1
70			3128.0		46.9	2.8	3215.7	0.0	31.2	3.5	3059.3		3063.1	
71	3048	(ir)	3127.7	−79.7	78.7	2.6	3215.5	−167.5	96.8	3.2	3059.1	−11.1	3062.9	−14.9
72			1544.6		0.0	2.7	1613.4		0.2	2.6	1548.4		1546.9	

TABLE 4: Continued

			BLYP				B3LYP				BLYP		B3LYP	
no.	a		b	c	d	e	b	c	d	e	f	g	f	g
73			1513.7		8.2	3.3	1581.1		0.2	3.1	1517.7		1518.2	
74	1493	(ir)	1484.4	8.6	340.4	5.0	1551.3	−58.3	287.9	4.5	1489.1	3.9	1492.4	0.6
75	1442	(ir)	1457.2	−15.2	11.7	2.1	1505.2	−63.2	15.8	2.0	1448.1	−6.1	1448.5	−6.5
76			1444.4		3.8	2.5	1503.5		3.5	2.8	1444.3		1447.0	
77	1426	(ir)	1434.8	−8.8	6.6	1.8	1488.4	−62.4	20.4	1.9	1430.0	−4.0	1430.1	−4.1
78	1366	(ir)	1371.2	−5.1	1.0	2.4	1411.1	−45.1	0.1	2.8	1362.8	3.2	1365.7	0.3
79	1326	(ir)	1333.3	−7.3	0.4	3.8	1374.9	−48.9	0.1	2.4	1331.1	−5.1	1329.1	−3.1
80	1276	(ir)	1278.4	−2.4	5.8	5.3	1318.7	−42.7	3.2	5.4	1277.6	−1.6	1271.7	4.3
81			1231.0		2.9	4.8	1275.6		1.6	5.4	1236.2		1232.6	
82	1223	(ir)	1212.0	11.0	16.8	5.5	1255.5	−32.5	2.4	5.3	1218.7	4.3	1217.9	5.1
83	1206	(ir)	1195.7	10.3	140.5	4.1	1244.1	−38.1	111.4	3.9	1208.2	−2.2	1204.7	1.3
84	1196	(ir,*)	1186.6	9.4	0.2	5.1	1234.8	−38.8	30.0	6.7	1192.9	3.1	1195.8	0.2
85		(*)	1179.6		85.4	7.1	1224.8		12.6	7.8	1182.0		1185.1	
86		(*)	1086.9	0.0	0.8	6.4	1117.7	0.0	1.4	3.7	1085.3	0.0	1083.2	0.0
87	1074	(ir,*)	1080.6	−6.6	17.6	9.9	1106.1	−32.1	16.9	11.6	1071.9	2.1	1070.1	3.9
88	1067	(ir,*)	1063.1	3.9	13.8	10.1	1090.4	−23.4	5.7	11.1	1057.5	9.5	1056.3	10.7
89	1047	(ir)	1052.6	−5.6	8.7	9.5	1079.7	−32.7	10.8	10.1	1039.9	7.1	1041.7	5.3
90		(*)	880.7		2.0	2.0	917.5		1.2	2.7	913.2		913.7	
91	911	(n)	864.7	46.3	0.0	7.0	910.5	0.5	0.3	6.4	903.6	7.4	910.4	0.6
92			855.3		27.1	2.4	893.6		1.5	9.6	887.5		89.35	
93			849.2		0.0	9.7	892.2		6.8	5.8	887.4		889.7	
94			845.3		0.0	9.5	887.9		4.9	8.7	883.3		883.2	
95	850	(ir,*)	815.5	34.5	91.5	2.7	852.3	−20.3	54.3	3.1	848.4	1.6	845.3	4.7
96	827	(ir,*)	789.7	37.3	84.4	2.4	831.7	−4.7	61.6	4.6	824.2	2.8	829.7	−2.7
97	821	(ir,*)	782.4	38.6	0.0	8.0	829.2	−8.2	28.9	7.0	817.6	3.4	813.3	7.7
98	808	(n,*)	764.7	43.3	0.0	10.6	806.4	1.6	1.5	11.4	799.1	8.9	806.3	1.6
99		(*)	761.6		0.0	11.2	803.1		0.3	11.3	795.9		803.1	
100	743	(n,*)	704.0	39.0	6.9	0.3	740.7	2.3	3.0	0.6	732.0	11.0	732.3	10.7
101			693.6		0.0	0.5	733.4		0.1	0.8	720.7		730.3	
102			689.0		0.3	0.4	731.1		0.3	0.5	716.9		716.0	
103	697	(R,*)	663.8	33.2	0.2	0.6	698.7	−1.7	2.9	9.6	689.2	7.8	698.4	−1.4
104	684	(n,*)	659.5	24.5	0.1	9.3	694.1	−10.1	0.6	1.9	682.4	1.6	684.1	−0.1
105	649	(n)	625.1	23.9	0.5	1.8	652.7	−3.7	0.9	1.8	643.5	5.5	642.8	6.2
106		(*)	577.6		3.5	6.5	606.3		2.5	1.6	603.6		605.0	
107	592	(n)	577.3	14.7	0.0	0.5	597.3	−5.3	5.4	6.9	599.4	−7.4	597.3	−5.3
108			573.5		0.1	6.2	594.6		0.8	6.4	597.4		594.5	
109			562.8		0.0	6.0	584.7		0.1	6.0	588.1		584.7	
110	565	(n)	541.0	24.0	0.0	5.7	564.7	0.3	0.1	5.9	565.4	−0.4	565.6	0.4
111	528	(n)	506.8	21.2	0.1	4.5	530.4	−2.4	1.0	4.7	529.6	−1.6	530.3	−2.3
112	475	(n,*)	452.1	22.9	0.0	3.5	478.3	−3.3	4.0	3.6	472.4	2.6	478.0	−3.0
113	444	(n)	434.4	9.6	2.4	5.6	445.2	−1.2	2.8	5.4	444.6	−0.6	438.8	5.2
114	375	(n,*)	344.5	30.5	0.0	5.0	369.8	5.2	0.2	4.9	360.0	15.0	369.5	5.5
115		(*)	342.4		3.2	1.0	355.0		2.1	0.7	354.1		351.2	
116	346	(n,*)	334.2	11.8	0.1	2.6	341.3	4.7	0.2	3.0	344.8	1.2	339.0	7.0
117	278	(n,*)	259.0	19.0	0.0	4.9	280.0	−20.0	0.0	4.8	270.6	7.4	280.0	−2.0
118	209	(n)	201.8	7.2	4.7	1.5	208.6	0.4	3.4	1.5	207.8	1.2	205.3	3.7
119	202	(n)	174.4	27.6	1.1	4.6	182.1	19.9	0.0	4.1	180.6	21.4	182.1	19.9
120			170.1			4.3	174.0		0.1	4.5	177.7		174.0	
121			93.9		0.0	3.1	97.7		0.0	3.1	98.1		97.7	
122			92.7		0.0	2.9	91.2		0.1	3.2	96.1		91.2	
123			36.6		0.0	3.2	45.4		0.0	5.6	38.2		45.4	
124			20.6		0.0	5.9	24.2		0.0	6.2	21.5		24.2	
125			20.5		0.0	5.0	20.1		0.0	5.0	21.2		20.1	
126			10.3		0.0	8.2	19.0		0.0	5.7	10.7		19.0	

mental and calculated frequencies. It does not come as a surprise that for systems of this complexity and low symmetry, the assignment can be subject to refiment for some time to come. In the reassignments, the careful match of experimental and calculated frequencies and intensities was pursued. It was also felt that it was legitimate to modify a tentative assignment when it led to improved convergence of the subsequent force fields fitting. We would like to mention that many of them are trivial and consist of moving up or down the normal mode number of a single vibration. Comparison of Tables 2, 3, and 4 of the present work with Tables 4, 5, and 6 of ref 5 is probably best left to the interested reader. The lack of spectra taken from well-characterized crystals with polarized light makes the present approach the only one viable to us. The relatively high accuracy of the DFT calculations ensures that we are a substantial step closer to the final vibrational assignment of these complicated systems. The present assignment was reached through a rather complicated iterative procedure that entailed three approaches: in the first a single scaling factor for all the frequencies is used, in the second the force constants are scaled individually or in sets, and in the third only part of the spectrum of frequencies is scaled. In the first approach, the scaling parameters are taken from the literature.[8,15] They are 0.994 for BLYP/6-31G* and 0.9613 for B3LYP/6-31G*. With these values, the overall standard deviations between experimental and calculated frequencies goes down by 3.5 cm^{-1} at the BLYP/6-31G* level and 47.3 cm^{-1} at the B3LYP/6-31G* level. The new values are therefore 31.8 and 22.1 cm^{-1}, respectively. They show that B3LYP/6-31G* calculations have a greater propensity to be scaled by a single overall factor.[15] The same deviations for the individual molecules go down by 5.0 and 53.4 cm^{-1} for α-2T, 3.2 and 46.2 cm^{-1} for α-4T, and 3.0 and 45.6 cm^{-1} for α-6T. Their final values are 33.4 and 23.6 cm^{-1} for α-2T, 31.3 and 21.9 cm^{-1} for α-4T, and 31.8 and 21.8 cm^{-1} for α-6T.

TABLE 5: Scaling Factors, χ_i, of the Internal Coordinates. The Standard Errors Are Reported in Columns a, b, and c for α-2T, α-4T, and α-6T Together with the Standard Deviations, σ (cm^{-1})

i	χ_i	a	b	c	
			BLYP/6-31G* (I)		
1	1.000	0.002	0.002	0.002	$C_\alpha C_\alpha$, $C_\alpha C_\beta$, HCC
2	0.978	0.002	0.002	0.002	CH, $C_\beta C_\beta$
3	1.045	0.003	0.003	0.002	CS, pyramidalizations, torsions
4	1.035	0.002	0.003	0.002	SCC, CCC, CSC
σ		8.3	9.2	9.4	
			B3LYP/6-31G* (II)		
1	0.952	0.002	0.001	0.001	$C_\alpha C_\alpha$, $C_\alpha C_\beta$, HCC
2	0.961	0.003	0.003	0.004	$C_\beta C_\beta$
3	1.000	0.001	0.002	0.002	CS, SCC, CCC, CSC, pyramidalizations, torsions
4	0.973	0.004	0.003	0.004	SCC, CCC, CSC
σ		6.9	7.8	8.3	

Although the procedure improves the overall agreement, one can quickly realize that the regions where the accuracy is greatest are actually worse off after scaling.

In the second approach, fitting of the scaling parameters was performed along standard lines.[15] The sets of internal coordinates employed here are the same as those of ref 5. Owing to the different nature of the methods, the grouping of the internal coordinates was different. It is found that both models require only four scaling parameters (see Table 5). Importantly, in both calculations, one of them is set to 1.00. Notice that this is not equivalent to having only three parameters because of the presence of off-diagonal elements that may still be scaled by the parameter of the other component. BLYP/6-31G* requires a scaling parameter of 1.00 for $C_\alpha-C_\alpha$, $C_\alpha-C_\beta$ stretches, and HCC bends; 0.978 for CH and $C_\beta-C_\beta$ stretches; 1.045 for CS stretches, pyramidalization, and torsional angles; and 1.035 for SCC, CCC, and CSC bends. B3LYP/6-31G* requires a scaling parameter of 1.00 for the CS stretch, SCC, CCC, and CSC bends, and pyramidalization and torsional angles; 0.952 for $C_\alpha-C_\alpha$, $C_\alpha-C_\beta$, and CH stretches; 0.961 for $C_\beta-C_\beta$ stretches; and 0.973 for HCC bends.

BLYP/6-31G* appears to be well suited to treat CC stretch force constants (notice, however, the exception of $C_\beta-C_\beta$). Also, the HCC force constants are well reproduced. B3LYP/6-31G* is most accurate for CS stretches, SCC, CCC, and CSC bends, and for pyramidalization and torsional angles. These tendencies quantify and detail the trends noticed before that were summarized noting that the region up to 1000 cm^{-1} is best simulated by B3LYP/6-31G* while the region between 1000−1600 cm^{-1} is best reproduced by BLYP/6-31G*. It is important to notice that in the BLYP/6-31G* calculations one of the most useful features of the Hartree−Fock calculations has disappeared, namely the consistent overestimate of all the frequencies which, in turn, requires scaling factors smaller than 1.00.

The two scaling procedures produce overall standard deviations between experimental and calculated frequencies that are down to 9.0 cm^{-1} at the BLYP/6-31G* level and 7.6 cm^{-1} at the B3LYP/6-31G* level. Similar deviations are found for the individual molecules. The corresponding values are 8.3 and 6.9 cm^{-1} for α-2T, 9.2 and 7.8 cm^{-1} for α-4T, and 9.4 and 8.3 cm^{-1} for α-6T.

The present analysis allows a third approach. This is the use of a single scaling factor for a small region where the agreement between experiment and theory is not satisfactory. We decided to scale the region up to 1000 cm^{-1} of the B3LYP/6-31G* calculations and the region between 1000−1700 cm^{-1} of the BLYP/6-31G* calculations. The two parameters were 1.0448 for BLYP/6-31G* and 0.9656 for B3LYP/6-31G*. If one excludes the CH stretches region, the two overall standard deviations were 8.30 and 6.68 cm^{-1}. At the BLYP/31G* level, the same values are 7.42 cm^{-1} for α-2T, 8.42 cm^{-1} for α-4T, and 8.77 cm^{-1} for α-6T, while at the B3LYP/6-31G* level they are 7.23 cm^{-1} for α-2T, 6.55 cm^{-1} for α-4T, and 6.60 cm^{-1} for α-6T.

4. Conclusion

In this work, we have used two models derived in the density functional theory context to calculate the molecular response to slow neutrons and infrared radiation for a series of oligomers of thiophene. It emerged that BLYP/6-31G* and B3LYP/6-31G* are complementary techniques. The highest accuracy of the former is in the region between 1000−1700 cm^{-1} while the highest accuracy of the latter is in the region below 1000 cm^{-1}. Both procedures give excellent agreement with the INS spectra whose intensity depends solely on the curvature of the potential energy surface at the minimum. They fail somewhat in the simulation of the infrared response of the two larger systems, a feature that can now be confidently ascribed to the dipole moment surface. In the future, it will be interesting to explore if similar problems are found for other extended systems and, when sufficient documentation is available, to try to determine the origin of this behavior. Analogously, it will be interesting to verify if the partial scaling of the vibrational frequencies that we have attempted here is general and if it can be applied to other systems. It is remarkable that for BLYP/6-31G* the use of a single scaling factor of 1.0448 in the region below 1000 cm^{-1} brings the standard deviation between observed and calculated frequencies down to 8.30 cm^{-1} (CH stretches are not included) and that the similar use of a single scaling factor of 0.9656 between 1000−1700 cm^{-1} for B3LYP/6-31G* produces a standard deviation of 6.68 cm^{-1}.

References and Notes

(1) Parr, R. G.; Yang, W. *Density Functional Theory of Atoms and Molecules*; Oxford University Press: New York, 1989.

(2) Wong, M. W. *Chem. Phys. Lett.* **1996**, *256*, 391.

(3) Marks, R. N.; Biscarini, F.; Zamboni, R.; Taliani, C. *Europhys. Lett.* **1995**, *32*, 523.

(4) Dodabalapur, A.; Torsi, L.; Katz, H. E. *Science* **1995**, *268*, 270. Dodabalapur, A.; Katz, H. E.; Torsi, L.; Haddon, R. C. *Science* **1995**, *269*, 1560.

(5) Degli Esposti, A.; Moze, O.; Taliani, C.; Tomkinson, J. T.; Zamboni, R.; Zerbetto, F. *J. Chem. Phys.* **1996**, *104*, 9704.

(6) Becke, A. D. *J. Chem. Phys.* **1988**, *88*, 1053.

(7) Becke, A. M. *J. Chem. Phys.* **1993**, *98*, 5648.

(8) Frisch, M. J.; Trucks, G. W.; Schlegel, H. B.; Gill, P. M. W.; Johnson, B. G.; Robb, M. A.; Cheeseman, J. R.; Keith, T.; Petersson, G. A.; Montgomery, J. A.; Raghavachari, K.; Al-Laham, M. A.; Zakrzewski, V. G.; Ortiz, J. V.; Foresman, J. B.; Cioslowski, J.; Stefanov, B. B.; Nanayakkara, A.; Challacombe, M.; Peng, C. Y.; Ayala, P. Y.; Chen, W.; Wong, M. W.; Andres, J. L.; Replogle, E. S.; Gomperts, R.; Martin, R. L.; Fox, D. J.; Binkley, J. S.; Defrees, D. J.; Baker, J.; Stewart, J. P.; Head-Gordon, M.; Gonzalez, C.; Pople, J. A. *Gaussian 94, Revision D.3*; Gaussian, Inc.: Pittsburgh, PA, 1995.

(9) Hehre, W. J.; Ditchfield, R.; Pople, J. A. *J. Chem. Phys.* **1972**, *56*, 2257. Hariharan, P. C.; Pople, J. A. *Theor. Chim. Acta.* **1973**, *28*, 213. Gordon, M. S. *Chem. Phys. Lett.* **1980**, *76*, 163.

(10) Hohenberg, P.; Kohn, W. *Phys. Rev.* **1964**, *B136*, 864. Kohn, W.; Sham, L. *J. Phys. Rev.* **1965**, *A140*, 1133.

(11) Becke, A. D. *Phys. Rev.* **1988**, *A38*, 3098.

(12) Lee, C.; Yang, W.; Parr, R. G. *Phys Rev.* **1988**, *B37*, 785.

(13) Vosko, S. H.; Wilk, L.; Nusair, M. *Can. J. Phys.* **1980**, *58*, 1200.

(14) Kearley, G. J. *J. Chem. Soc., Faraday Trans. 2* **1986**, *82*, 41. Kearley, G. J. *Spectrochim. Acta* **1992**, *48A*, 349.

(15) Rauhut, G.; Pulay, P. *J. Phys. Chem.* **1995**, *99*, 3093.

(16) Jobic, H.; Ghosh, R. E.; Renouprez, A. *J. Chem. Phys.* **1981**, *75*, 4025.

(17) Howard, J.; Ludman, C. J.; Waddington, T. C.; Tomkinson, J. *Chem. Phys.* **1980**, *46*, 361.

(18) Horowitz, G.; Bachet, B.; Yassar, A.; Lang, P.; Demanze, F.; Fave, J.-L.; Garnier, F. *Chem. Mater.* **1995**, *7*, 1337.